Influence of Solid Solution Formation on Polarity: Molecular Modeling Investigation of the System 4-Chloro-4′-nitrostilbene/4,4′-Dinitrostilbene

C. Gervais, T. Wüst, and J. Hulliger*

Department of Chemistry and Biochemistry, University of Berne, Freiestrasse 3, CH-3012 Berne, Switzerland

Received: February 2, 2005; In Final Form: April 15, 2005

Growth-induced polarity formation in solid solutions composed of dipolar 4-chloro-4′-nitrostilbene molecules and nonpolar 4,4′-dinitrostilbene molecules was investigated by means of two molecular modeling procedures. Calculation of the mixing energy in the *bulk structures* predicted solid solution formation within the whole composition range. Computation of the interaction energies present at *growing surfaces* allowed the distribution coefficient as well as the fraction of dipoles in either the up or down orientation to be calculated by a mean-field model. Miscibility and polarity were found to vary for the faces (*hkl*) investigated, leading to crystals composed of sectors with different compositions and polarities. The present study highlights the fact that a solid solution crystal may not be a homogeneous entity and that surface effects arising during slow growth can have an impact on solid state properties.

Introduction

In mixed crystals, chemical compositions in the bulk may be significantly affected by mechanisms taking place at the crystal−nutrient interface. This phenomenon is widely investigated because of its direct impact on the physical and chemical properties of the material. While an abundant amount of literature is dedicated to theoretical and experimental studies of surface segregation in atomic alloys,[1−4] only a limited number of papers deals with molecular compounds.[5−7] In the case of mixed crystals of polar molecules, it was observed that inclusion of impurities in a centrosymmetric host matrix was responsible for the appearance of significant second-order nonlinear optical properties.[8] Surface effects giving rise to polar properties were also observed in single-component systems of dipolar molecules, classified as centrosymmetric by X-ray diffraction.[9,10] In the past decade, a growth model has been developed to quantify such a phenomenon, called *growth-induced polarity formation*, for systems composed of dipolar molecules A−π−D (A and D represent acceptor and donor terminals, respectively; π represents a delocalized π-electron system ensuring a significant dipole moment ($\vec{\mu}$) pointing from A to D). Principally, it can be explained as follows: Upon growth, a 180° orientational disorder of dipoles can arise at the surface due to significant probabilities for attaching molecules, forming, for example, A···A or D···D instead of A···D interactions with previously attached molecules. Different probabilities (P_{AA} and P_{DD}) lead to different ratios of molecules in state *up* and *down* (i.e., the projection of the molecular dipoles along the growth direction are ↑ and ↓, respectively) and thus to the appearance of polarity for the face considered. In the case of elongated prolate-type molecules, a 180° molecular flipping in the bulk is not likely (high activation energy), so that polarity arising at the surface leads to a metastable polar state for the bulk.

Because the attachment probabilities (P_{AA}, P_{DD}, and P_{AD}) are directly related to the intermolecular interaction energies involved at the surface,[11,12] a computational study based on energy calculations can be used to quantify polar effects. Such an investigation was recently carried out to calculate growth-induced polarity in crystals of 4-chloro-4′-nitrostilbene (CNS). By means of force-field methods, calculation of the intermolecular interaction energies present at the different surfaces allowed the appearance of polarity for *b* sectors of {011} faces to be predicted, a result confirmed both by phase-sensitive second-harmonic microscopy and by scanning pyroelectric microscopic measurements.[13]

Here, in a logical continuation, the study is extended to a two-component system composed of CNS and 4,4′-dinitrostilbene (DNS). Two questions are discussed: (i) What is the miscibility range between CNS and DNS? (ii) What is the impact of the formation of solid solutions between nonpolar molecules (DNS) and dipolar molecules (CNS) on polarity (in consideration that both pure components crystallize in centric structures)? These issues already received a brief answer in ref 14; that is, an experimental study confirmed a full range solid solution for $CNS_{1-X}DNS_X$ ($0 < X < 1$) and a second-harmonic generation effect for mixed crystals (*c*-plate) was observed. However, a thorough theoretical investigation of the CNS/DNS system was missing so far.

In the present paper, question (i) is addressed from two different points of view: (1) *Miscibility in the bulk* of the two components. A molecular modeling procedure is proposed in which solid solutions based on the 3D crystal structures of CNS and DNS are constructed and optimized and their lattice energy is calculated. Probabilities to form solid solutions are estimated according to the excess of energy due to the mixing of the two components in the solid. (2) *Miscibility on the growing faces*, that is, CNS/DNS ratios at the surfaces. For that purpose, the following procedure to investigate the influence of solid solution formation on *growth-induced polarity* (issue (ii)) is applied: (a) determination of the solid solution range for $CNS_{1-X}DNS_X$ by using force-field methods; (b) calculation of all possible interaction energies between a reference molecule in the bulk and its first nearest neighbors; (c) selection of the relevant interaction energies present at the surface of the growing faces (*hkl*); (d) use of these energies in a generalized Markov-type model[15] to predict polarity and miscibility for faces (*hkl*).

1. Structures

1.1. CNS and DNS Structures. The present study is performed on the basis of the CNS and DNS crystal structures

* To whom correspondence should be addressed. E-mail: publication.hulliger@iac.unibe.ch.

10.1021/jp0505835 CCC: $30.25
Published on Web 06/08/2005

described in ref 14. DNS: $P2_1/c$, with $a = 3.818(6)$ Å, $b = 13.007(2)$ Å, $c = 12.478(2)$ Å, and $\beta = 94.371(2)°$. CNS: $P2_1/c$, with $a = 3.837(1)$ Å, $b = 12.916(2)$ Å, $c = 12.221(3)$ Å, and $\beta = 93.91(3)°$. CNS molecules are positioned onto the center of symmetry, leading to an occupancy of 50%:50% *on average* for A (NO_2) and D (Cl) terminal groups and thus a 50%:50% distribution of dipoles in state *up* and *down*. Recently, a reinvestigation of the crystal structure by X-ray diffraction of CNS single crystals grown from toluene led to the same packing arrangement but with a different distribution of the two orientational states (40%:60%, space group $P1$). The difficulty to determine doubtlessly the proportion of up and down molecules in the bulk is due to the phenomenon of polarity formation observed and predicted for pure crystals of CNS,[13] leading to crystal sectors showing different distributions (up/down).

1.2. Prediction of Solid Solution Formation. Prediction of *bulk* solid solution formation in the CNS/DNS system was performed by using the molecular modeling method described in ref 16. The procedure consists of constructing artificial three-dimensional solid solutions (S_i, with i = CNS, DNS) generated from either the CNS or the DNS crystal packing, respectively. After full optimization of the solid solutions (i.e., molecules and unit-cell parameters are allowed to relax), the excess of energy ($\Delta E^i_{\mathrm{mix}}$) induced by the mixing of the two components is calculated; for details, see Appendix A. By looking at the variation of $\Delta E^i_{\mathrm{mix}}$ with the ratio X_{bulk} of DNS molecules, one can draw a conclusion about the stability and thus about the chances to observe mixed structures. For instance, $\Delta E^i_{\mathrm{mix}}$ close to zero for the whole range of X_{bulk} is expected to give an ideal solid solution, while a large positive $\Delta E^i_{\mathrm{mix}}$ value for whatever X_{bulk} is representative of a nonmixing of the two compounds (eutectic behavior) in a structure of type S_i. This method based on ΔE_{mix} may be related to the theory of solid solution developed by Bragg and Williams[17] and Gorsky,[18] which qualitatively predicts the formation of solid solution A_xB_{1-x} according to an interaction parameter (W) defined as the difference of energy between contacts of AA, BB, and AB entities.

The number of possible molecular arrangements (configurations) in the bulk depends on the size of the supercell, the ratio CNS/DNS (X_{bulk}), and the ratio up/down of CNS molecules. To simulate correctly the randomness inherent to a solid solution, a sufficiently large supercell has to be defined ($a \times b \times c = 6 \times 3 \times 3$, i.e., 108 molecules). For a representative average value of ΔE_{mix}, for each ratio $X_{\mathrm{bulk}} = [0.1, 0.2, \ldots, 0.9]$, only 30 supercells with different configurations of CNS up/down and DNS molecules were chosen randomly in view of a huge number of possible molecular arrangements. This is justified by our finding that the lattice energy depended mainly on the ratio up/down of CNS molecules and not on the spatial distribution of CNS up, CNS down, and DNS. Moreover, this number of supercells is considered sufficient because the ratio up/down was restricted to stay within the range from 45%:55% to 55%:45%.

Solid solution and single-component structures were optimized and lattice energies computed by using the consistent force field Compass[19] with Ewald summation for both Coulombic and van der Waals interactions. The strong similarity between the two structures of CNS and DNS gave identical crystallographic parameters and energy values for solid solutions S_{CNS} and S_{DNS}, within statistical deviations. Mixing energies for S_{CNS} are shown in Figure 1.

Whatever the ratio between CNS and DNS was, constructed solid solutions showed values for ΔE_{mix} near zero, indicating that *solid solutions close to ideality are expected to be found for the whole range of* X_{bulk}. This can be explained by considering ΔE_{mix} as the enthalpy of mixing (ΔH_{mix}): for an ideal solid solution with $X_{\mathrm{bulk}} = 0.5$, the entropy of mixing (ΔS_{mix}) is $R \ln 2$.[20] To keep the free energy of mixing $\Delta G_{\mathrm{mix}} = \Delta H_{\mathrm{mix}} - T\Delta S_{\mathrm{mix}}$ within the range of thermal energy RT (indicating that mixing between the two compounds is thermodynamically possible), the mixing enthalpy (ΔH_{mix}) has to be lower than about 4 kJ/mol at a temperature of $T = 300$ K. This condition is fulfilled in our case (for other ratios than 0.5, similar arguments hold).

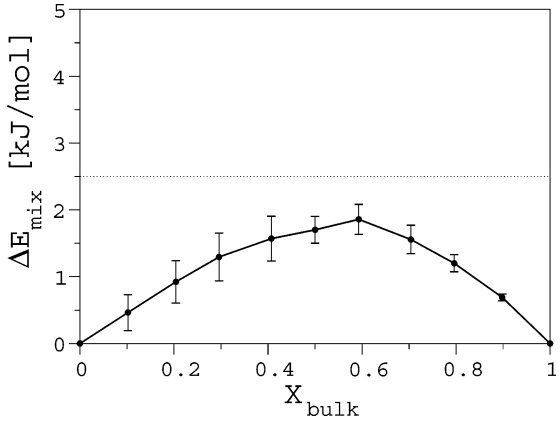

Figure 1. Excess energy (ΔE_{mix}, kJ/mol) for constructed solid solutions as a function of the molar fraction (X_{bulk}) of DNS molecules. Vertical bars indicate statistical errors of the energies resulting from the variation of the ratio up/down of CNS molecules in the range from 45%:55% to 55%:45%; see text. Thermal energy ($RT \approx 2.5$ kJ/mol at $T = 300$ K) is indicated by a dotted line for comparison purposes.

It has to be emphasized that a prediction is limited to the crystal packings (S_i) investigated, so that a conclusion cannot be directly extended to other types of crystal structures. However, in the present case, the structures of CNS and DNS are similar ($S_{\mathrm{CNS}} \sim S_{\mathrm{DNS}}$) and no polymorphism for the pure compounds has been observed so far. It is therefore likely that application of the procedure to the known crystal packings of CNS and DNS is sufficient to draw general conclusions about *their miscibility in the bulk*.

Note that this procedure deals with a thermodynamic state of the mixed crystals. It does not take into account surface effects, such as an asymmetry at surfaces leading to a distribution of the two components which varies according to the site and the face considered.[6,7] On the contrary, the Markov model presented below allows the ratio CNS/DNS to be calculated at grown surfaces, so that both methods can be seen as complementary (bulk and surface).

2. Molecular Modeling Study for Slowly Growing Faces

To quantify surface effects on solid solution formation and growth-induced polarity, one needs to know the interaction energies for the molecule being attached to the surface. Hereafter, all possible interaction energies between a molecule in the bulk and its first neighborhood are calculated. The morphology of mixed crystals is analyzed to define the predominant faces (hkl) and those neighbors which are present at corresponding surfaces. A generalized Markov mean-field model is then applied for investigating both growth-induced polarity and the ratio CNS/DNS separately for each face.

2.1. Interaction Energies. Pairwise interaction energies in the CNS/DNS system were calculated according to the procedure described in ref 13. The calculation was limited to interactions including only first nearest neighbors, which have shown to be the determining contributions for polarity and miscibility

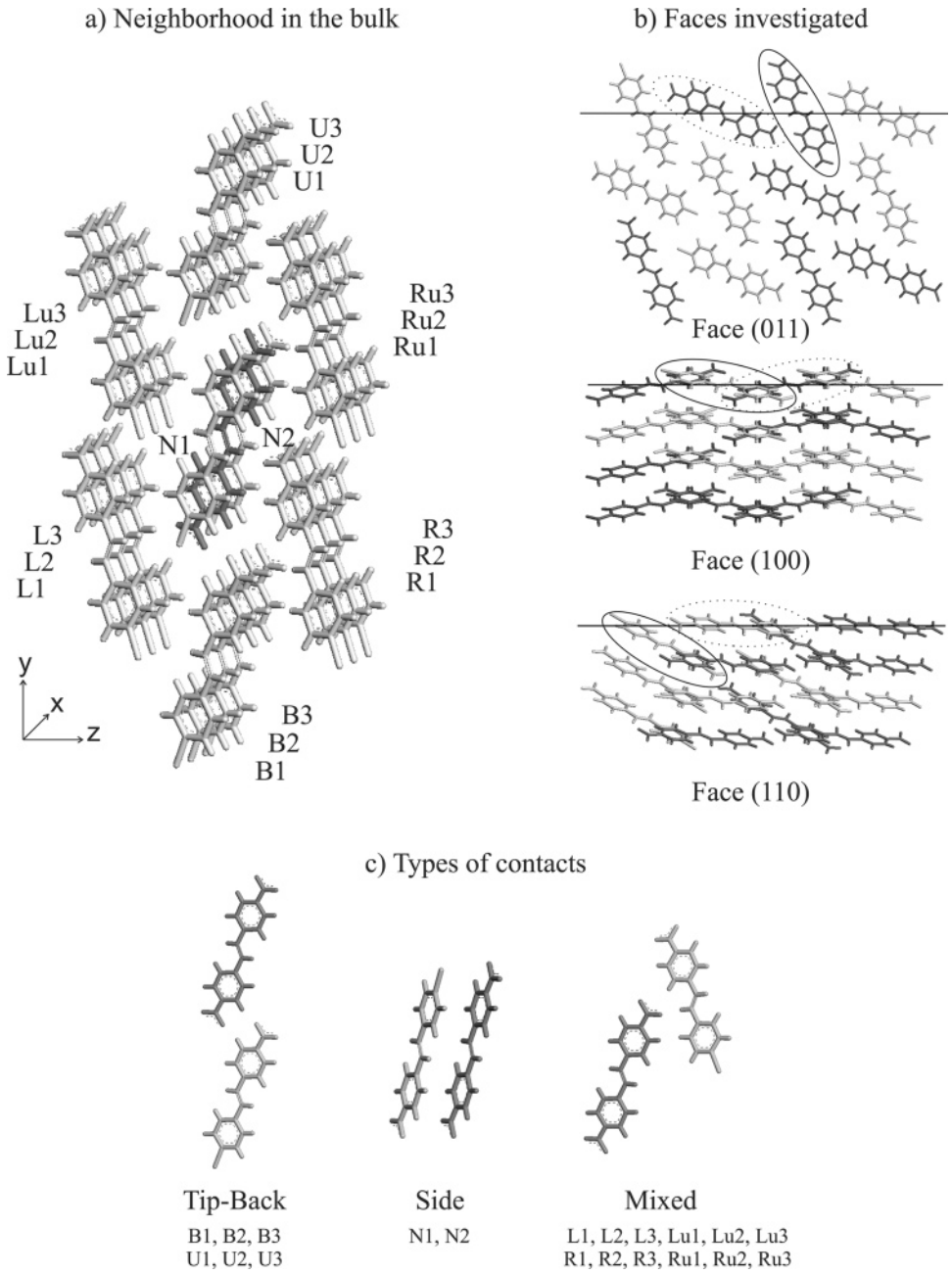

Figure 2. (a) Neighborhood of a reference molecule in the bulk. The 20 neighbors are designated by a label giving their position relative to the reference molecule. Here, the reference molecule is DNS (nonpolar), being surrounded by CNS neighbors in the state up. This system was used to calculate the energies E^i_{nu}, with *i* labeling the neighbor considered (see text). (b) Faces of the solid solutions investigated. Here, faces are extracted from a solid solution with a CNS/DNS ratio of 50%:50%. Ellipsoids indicate the two different sites g =I (solid) and g =II (dotted) emerging on the surface. (c) Classification of the neighbors according to their type of contacts with the reference molecule. For all figures, CNS molecules are colored in light gray and DNS molecules in dark gray.

in this system. Besides, only interactions in the CNS packing were calculated, this because of a strong similarity between CNS and DNS structures. It is likely that coupling energies found in the DNS packing are almost equal and thus give similar results for the properties investigated. (This point is justified by a study on CNS[13] in which no, partial, or full optimization of the CNS structures was performed prior to energy calculation. The three sets of energies were found to be similar and gave identical results for polarity.) Finally, pair interactions were assumed to be independent of the state of other neighbors.

Figure 2a shows a reference molecule surrounded by $\lambda_T = 20$ first nearest neighbors in the bulk. Neighbors can be classified according to their type of interactions (tip−back, side, or mixed; see Figure 2c). Both reference and neighbor molecules can be DNS (nonpolar), CNS (polar state up), or CNS (polar state down), with polar states up and down being given with respect to the projection of the dipoles along the $+b$ axis. Therefore, each of these pair interactions (see Figure 2) leads to nine different interaction energies. That is, a total number of $3 \times 3 \times \lambda_T = 180$ energies was thus calculated.

Energies were computed by using the consistent force field Compass with group-based cutoffs (group defined as the entire molecule) for both Coulombic and van der Waals interactions. The cutoff distance was set to 60 Å (spline width 20 Å, buffer width 8 Å, van der Waals tail correction 60 Å) in order to ensure the convergence of the energy values.

Energy calculations have confirmed the center of symmetry present in this structure, since only marginal errors (less than

TABLE 1: Interaction Energies [kJ/mol] between a Reference Molecule and Its 20 Nearest Neighbors in the Bulk, Calculated for $T = 0$ K[a]

i	E^i_{dd}	E^i_{ud}	E^i_{nd}	E^i_{nu}	E^i_{du}	E^i_{uu}	E^i_{dn}	E^i_{nn}	E^i_{un}
B1	−1.1	−0.7	−1.0	−1.9	−1.8	−1.1	−1.9	−1.9	−1.0
B2	−5.4	−3.9	−5.4	−9.1	−8.9	−5.4	−9.1	−9.3	−5.4
B3	−4.5	−3.7	−4.5	−8.1	−7.9	−4.5	−8.1	−8.3	−4.5
U1	−4.5	−7.9	−8.1	−4.5	−3.7	−4.5	−4.5	−8.3	−8.1
U2	−5.4	−8.9	−9.1	−5.4	−3.9	−5.4	−5.4	−9.3	−9.1
U3	−1.1	−1.8	−1.9	−1.0	−0.7	−1.1	−1.0	−1.9	−1.9
N1	−19.4	−22.5	−19.6	−19.3	−21.9	−19.4	−19.3	−16.4	−19.6
N2	−19.4	−21.9	−19.3	−19.6	−22.5	−19.4	−19.6	−16.4	−19.3
L1	−1.8	−1.6	−1.8	−1.8	−1.6	−1.7	−1.5	−1.6	−1.5
L2	−6.1	−6.4	−6.3	−5.8	−4.7	−5.3	−4.6	−5.5	−5.1
L3	−3.6	−3.9	−3.8	−8.2	−7.1	−7.6	−6.9	−7.9	−7.4
Lu1	−1.8	−1.6	−1.5	−1.5	−1.6	−1.7	−1.8	−1.6	−1.8
Lu2	−6.1	−4.7	−4.6	−5.1	−6.4	−5.3	−6.3	−5.5	−5.8
Lu3	−3.6	−7.1	−6.9	−7.4	−3.9	−7.6	−3.8	−7.9	−8.2
R1	−7.6	−3.9	−7.4	−6.9	−7.1	−3.6	−8.2	−7.9	−3.8
R2	−5.3	−6.4	−5.1	−4.6	−4.7	−6.1	−5.8	−5.5	−6.3
R3	−1.7	−1.6	−1.5	−1.5	−1.6	−1.8	−1.8	−1.6	−1.8
Ru1	−7.6	−7.1	−8.2	−3.8	−3.9	−3.6	−7.4	−7.9	−6.9
Ru2	−5.3	−4.7	−5.8	−6.3	−6.4	−6.1	−5.1	−5.5	−4.6
Ru3	−1.7	−1.6	−1.8	−1.8	−1.6	−1.8	−1.5	−1.6	−1.5

[a] Energies are labeled E^i_{rv}, where r and v denote the state up (u), down (d) or nonpolar (n) of the reference molecule and the neighbor molecule, respectively. i labels the neighbor. The neighbors are gathered according to their type of contact with the reference molecule (tip−back, side, or mixed) to highlight the center of symmetry relating all the energy values in the bulk. For notation of the neighbors and types of interactions, see Figure 2a,c.

0.05 kJ/mol) were found between energies of the same type (tip−back, side, or mixed).

As seen in Table 1, energy values depend strongly on the type of interaction, the relative position, and the state (up, down, or nonpolar) of molecules. The strongest contacts are side interactions taking place between the reference molecule and the neighbors N1 or N2, because of the presence of π-stacking. Besides, some pairwise interactions are particularly selective toward the polar state up or down of a CNS reference molecule. For instance, $E^{B2}_{ud} > E^{B2}_{dd}$ and $E^{B2}_{uu} > E^{B2}_{du}$, indicating that the CNS neighbor B2 makes a preferential interaction with a CNS reference molecule in state down whatever its own state. Similarly, selectivity toward the chemical nature of the reference molecule can be found. (See for instance the DNS neighbor N1 (or N2), which makes stronger interactions with a CNS reference molecule than with DNS (E^{N1}_{dn}, $E^{N1}_{un} < E^{N1}_{nn}$).)

Such anisotropies have no consequence in the bulk, since the center of symmetry between the interaction energies cancels out any preference for a polar reference molecule to be in state up or down. However, this is not true for the crystal surface where some interactions of the bulk are not present anymore. *The breaking of symmetry at the surface and the strong anisotropy between the different types of interaction energies (e.g., B2 above) are the fundamental causes for the appearance of growth-induced polarity*. Miscibility between the two compounds may result because of a difference of energy when inserting a CNS or DNS molecule in a given environment (e.g., N1) so that it is likely that the distribution CNS/DNS will depend on the face considered.

2.2. Determination of Relevant Faces (*hkl*) for Polarity Formation. The morphology of CNS crystals was investigated experimentally and by molecular modeling methods in ref 13. Three families of faces were found, namely, the faces {011} (predominant faces which account for ∼79% of the total surface area (A) of the crystal), the faces {100} ($A \sim 11\%$), and the faces {110} ($A \sim 5\%$), which were predicted but not observed by goniometric measurements. A needle shape was also observed for CNS crystals grown from less polar solvents (ethanol and toluene) or from vacuum as well as for DNS crystals and mixed crystals $CNS_{1-X}DNS_X$. Therefore, it is expected that the morphology of CNS crystals is representative for those found in the CNS/DNS system. Hereafter, the ratio CNS/DNS at the surface and growth-induced polarity formation were investigated for three representative faces: (011), (100), and (110). Even though the face (110) was not observed experimentally, it was studied here for comparison purposes as well.

As a result of the broken symmetry, two principally different molecular environments manifest on the surface of each face (see Figure 2b). These two sites $g = \mathrm{I}, \mathrm{II}$ have to be treated separately in the analytical description (see below).

2.3. Application of a Generalized Markov Mean-Field Model. Polarity formation and miscibility arising during the growth of a face (*hkl*) are described by means of a generalized Markov mean-field model; see refs 13 and 15. In this model, the crystal is assumed to grow layer-by-layer; that is, a new layer starts to grow only when the previous layer is completed. Previously grown layers are kept frozen; that is, molecules in the bulk are not allowed to flip. Growth is considered from the gas phase composed of a constant fraction (X_{gas}) of DNS molecules. Molecules in the solid are represented by building blocks in state up, down, and nonpolar corresponding to CNS molecules in state up, CNS molecules in state down, and DNS molecules, respectively.

Within the present model, evolution of the system in terms of polarity formation and miscibility is fully determined by the different attachment probabilities for docking molecules on the surface. Probabilities are given by normalized Boltzmann factors taking into account the molecular neighborhood within a mean-field estimate. For further details, see Appendix B. In the asymptotic limit of growth, two quantities are defined:

(1) The difference between the molar fractions of CNS molecules in state up and down on the surface. This is defined by

$$X_{net} = \frac{X^{I}_{d} + X^{II}_{d}}{2} - \frac{X^{I}_{u} + X^{II}_{u}}{2}$$

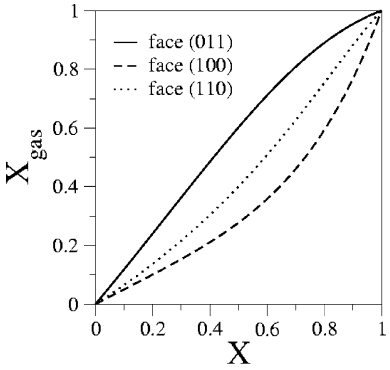

Figure 3. Molar fraction (X) of DNS molecules in the as grown solid with respect to X_{gas}, for the three faces (011), (100), and (110). Temperature $T = 300$ K. The analysis shows clearly that the distribution coefficient ($k = X/X_{gas}$) can vary from face to face.

where X_d^g and X_u^g denote the molar fractions of CNS molecules in state down and up on surface sites g = I, II, respectively.

(2) The molar fraction of DNS molecules on the surface (X is defined for a specific face (*hkl*) and has to be differentiated from the ratio X_{bulk} of DNS molecules calculated for the bulk structure (see section 1.2)):

$$X = 1 - \left(\frac{X_d^I + X_d^{II}}{2} + \frac{X_u^I + X_u^{II}}{2}\right)$$

The number of layers before reaching the asymptotic state is generally negligible in comparison to the total number of layers which can be found in a real crystal, so that the parameters calculated here at the surface can be extended to a large part of the growth sector of the face (*hkl*).

2.4. Results. *2.4.1. Miscibility between CNS and DNS.* Miscibility between the two components is studied by looking at the variation of X with X_{gas} (see Figure 3).

The ratio between CNS and DNS for a given X_{gas} depends on the face investigated. For the faces (100) and (110), the amount of DNS molecules is higher in the solid than in the gas phase, indicating a preferential insertion of DNS. This is particularly the case for the face (100) in which a strong deviation from the diagonal $X = X_{gas}$ is observed (e.g., $X_{gas} = 0.5$, $X = 0.73$). On the contrary, the environment at the surface of the face (011) is slightly in favor of the CNS insertion ($X < X_{gas}$). This selectivity becomes larger with higher fractions X_{gas}.

It is obvious that the procedure applied here is not intended to give quantitative results for the miscibility between the two components such as it can be found in a binary phase diagram. Several reasons could be invoked: Some are intrinsic to the growth model (e.g., assumption of a layer-by-layer growth close to equilibrium, no kinetic effects taken into account, only a few degrees of freedom for molecules allowed), to the calculation of the energies (e.g., force-field method, and thus made at 0 K, no vibrational energy taken into account, charge distribution of NO_2 and Cl groups considered as isotropic), or to other effects such as the presence of dislocations. Nevertheless, the present model can be used to make a qualitative estimation of the miscibility, which in the case of CNS/DNS was found for the whole range of X. Moreover, the model confirms that *miscibility between the two components varies for the different faces*.

2.4.2. Growth-Induced Polarity Formation. Evolution of polarity is investigated by looking at the variation of X_{net} with X (see Figure 4, left).

The face (100) shows no polarity irrespective of X. This is a result of the presence of a center of symmetry at the surface between sites I and II:[13] Even if an unequal up/down ratio is observed on one site (e.g., 40%:60%), the reverse ratio will be found for the other site (60%:40%), therefore leading to a total polarity of zero. The faces (011) and (110) show similar polar behaviors: For $X < 0.2$, $X_{net} \approx -0.5$ (both faces), which corresponds to an up/down ratio of 75%:25%. For $X > 0.2$, polarity decreases rapidly toward 0.

From a schematic point of view, the polar behavior observed for the faces (011) and (110) can be explained by *a coupled selectivity* of CNS *and* DNS molecules[21] toward the insertion of CNS molecules in state up. At $X = 0$, faces are composed uniquely of CNS molecules which tend to attach on the surface preferentially in state up (for a detailed study of this phenomenon, see ref 13). In the case of solid solutions ($X > 0$), two effects compete with each other: (i) The presence of DNS molecules on the surface favors the insertion of CNS molecules in state up so that the deviation from an up/down ratio of 50%:50% increases. (ii) The increasing number of DNS molecules reduces the total amount of CNS molecules in the solid, and thus, macroscopic polarity X_{net} decreases. For small X values, effects (i) and (ii) balance each other, leading to a constant X_{net}, while effect (ii) becomes predominant for large X values.

3. Discussion

Comparison between miscibility and polarity obtained from the *bulk* structure or the *individual grown faces* is exemplified by looking at a solid solution grown at $X_{gas} = 0.5$ and $T = 300$ K.

While the bulk miscibility between CNS and DNS could be estimated in section 1.2, a quantification of the solubility requires experimental measurement of the phase diagram.[22] This would

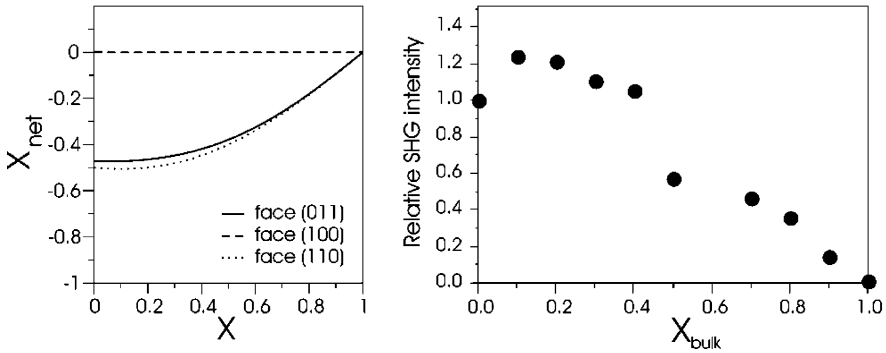

Figure 4. Comparison between the polarity (X_{net}) and the SHG effect observed for mixed crystals. Left: X_{net} vs molar fraction (X) of DNS molecules in the as grown solid, calculated by the generalized Markov mean-field model at $T = 300$ K. Results are shown for the three faces (011), (100), and (110). Right: relative intensity of SHG signals measured for mixed crystals grown from the melt (arbitrary scale fixed to 1 for pure CNS crystals). The right figure is adapted from ref 14.

TABLE 2: Neighborhood {*i*} for a Reference Molecule on Site I or II for the Three Faces Investigated[a]

(*hkl*)	λ	*g*	neighbors {*i*} from *g*	neighbors {*i*} from *g*′
(011)	14	I	B1 B2 B3 N1 N2	L1 L2 L3 Lu1 Lu2 Lu3 R1 R2 R3
		II	B1 B2 B3 N1 N2	L1 L2 L3 Ru1 Ru2 Ru3 R1 R2 R3
(100)	13	I	B1 U1 N1 B2 U2	L1 Lu1 R1 Ru1 L2 Lu2 R2 Ru2
		II	B3 U3 N2 B2 U2	L3 Lu3 R3 Ru3 L2 Lu2 R2 Ru2
(110)	12	I	B1 B2 B3 N1	L1 L2 R1 R2 L3 R3 Lu1 Ru1
		II	B1 B2 B3 N2	L2 L3 R2 R3 L1 R1 Lu3 Ru3

[a] Neighbors may belong to the same site (*g*) as the reference molecule or to the other site (*g*′). λ corresponds to the number of first nearest neighbors present on the surface ($\lambda_T = 20$ in the bulk).

TABLE 3: Molar Fraction (*X*) of DNS Molecules and Polarity (X_{net}) Found for Different Faces (*hkl*) of an as Grown Solid Solution ($X_{gas} = 0.5$, $T = 300$ K)

structure	*X*	X_{net}
face (011)	0.41	−0.41
face (100)	0.73	0
face (110)	0.59	−0.34

give for $X_{gas} = 0.5$ a single average bulk CNS/DNS ratio. On the contrary, significantly different CNS/DNS ratios are obtained during the growth process of the different faces (see Table 3). Generally, the diffusion rates of molecules within a crystal are very low, and as said previously, the 180° flipping of the stilbene molecules in the bulk is not likely. Therefore, it is not expected that *X* values found for the different faces equilibrate upon time, leading to a statistical distribution of CNS and DNS molecules over the entire crystal. Consequently, the crystals will show a heterogeneous distribution of CNS and DNS molecules between sectors corresponding to the different faces (*hkl*). Indeed, the crystal can be decomposed into six cone-shaped growth sectors, with four belonging to the family {011} and two to the family {100} (the faces {110} are not considered here; see Figure 5).

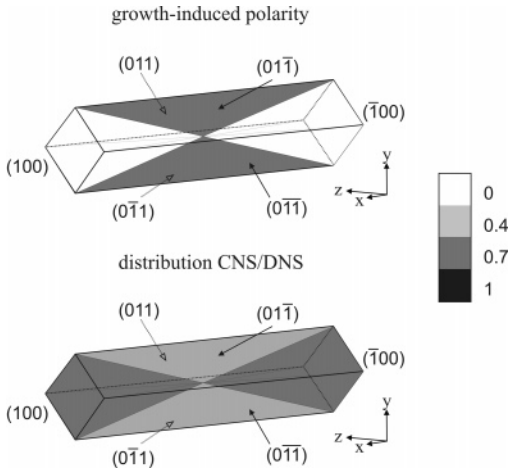

Figure 5. Geometrical decomposition of a mixed crystal composed of CNS and DNS molecules into four growth sectors {011} and two growth sectors {100}. Gray scales indicate $|X_{net}|$ (absolute value of growth-induced polarity, above) and *X* (molar fraction of DNS molecules in the crystal, below) for each growth sector of a solid solution at $X_{gas} = 0.5$ and $T = 300$ K.

The same *X* value is expected to be found for all faces of a given family because their surfaces show identical environments. The average of the different *X* values weighted by the volume of their corresponding growth sector results in an average fraction of DNS molecules of 0.57 for the whole crystal, a value which may be used for comparison with experiments.

The analysis applied to the bulk structure yields no polarity because of the center of symmetry we have anticipated, leading therefore to an equal distribution between CNS molecules in state up and in state down, respectively. However, macroscopic polarity arises during the growth on the faces (011) and (110) due to the disappearance of this symmetry at the surface. (For the face (100), no polarity arises; see above.) Similar arguments to those given above for *X* apply for the distribution of X_{net}; that is, a metastable state is expected to be found with different up/down ratios of CNS molecules belonging to the different growth sectors. The center of symmetry relating the different growth sectors of a same family leads to a crystal with an average CNS/DNS ratio of 50%:50%, nevertheless yielding net polarity in sectors {011}. An excess of CNS molecules in state up on these faces produces surfaces in which the majority of CNS molecules point their Cl groups toward the nutrient. For comparison with experiments, SHG effects measured on powder samples[14] were compared with X_{net} values calculated for the face (011). Figure 4 shows that theoretical predictions are in good agreement with experiments, since the same qualitative behavior was found in both cases, that is, nonzero polarity for pure CNS crystals and the presence of a flat maximum for small fractions of DNS, followed by a decrease of polarity toward zero.

More precise predictions of polarity in real crystals may hardly be achieved because of other factors affecting the growth as well as restrictions in the model (see section 2.4.1). Besides, difficulties may arise when considering that polarity can be expressed in an experimental crystal by different ways, for example, by a SHG or a pyroelectric effect. Here, prediction was based only on the orientation of the dipoles, while multipole effects were not taken into account.

Summary and Conclusion

Solid solution formation and growth-induced polarity formation in the CNS/DNS system was investigated by two different routes using molecular modeling methods: By the first one, just the bulk structure was considered, while the second one focused on the specific molecular environments at different growing crystal faces. Specifically, the first study consisted of calculating the lattice energies of the bulk structures of CNS, DNS, and the modelized solid solutions. The excess of energy due to the mixing of the two compounds in the solid was found to be rather low, indicating that CNS and DNS can form solid solutions within the entire range of composition. Due to the center of symmetry, polarity cannot arise within this approach. The second method allowed a prediction of miscibility between CNS and DNS as well as growth-induced polarity formation for the faces (011), (100), and (110). An analytical description taking into account details of the molecular neighborhoods at a surface in terms of interaction energies allowed *X* and X_{net} to be calculated for each face individually. Inhomogeneous distributions of CNS and DNS molecules as well as nonequal up/down ratios for CNS were obtained for the different growth sectors investigated.

The anisotropic spatial distribution of CNS up, CNS down, and DNS into different growth sectors is a fundamental issue

which raises general questions. First, it highlights the fact that a crystal structure determined by X-ray diffraction is based on *average* positions of molecules. As a result, X-ray single-crystal data may in particular cases not be appropriate to explain observed physical properties. Second, the prediction of structures and their properties is often based on three-dimensional bulk procedures. However, the fact that crystals grow from the surface may influence both the packing and composition. The studies in refs 5, 7, and 8 provide instructive examples for the importance of surface effects. Growth-induced polarity formation is another mechanism leading to a property inherently induced by the fact that crystals grow. Therefore, it might not always be sufficient to perform predictions for a solid state without considering the crystal as grown from surfaces in contact with an environment.

Acknowledgment. We acknowledge the Swiss National Science Foundation (Project No. 200021-101658/1) for financial support and Accelrys for providing computational tools.

Appendix

A. Procedure for the Prediction of Solid Solution Formation. *Construction of Solid Solutions.* Two types of solid solutions were constructed, namely, S_{CNS} and S_{DNS}, based on the CNS and DNS crystal structures, respectively. To obtain S_{CNS}, the CNS structure was extended to a supercell, $a \times b \times c = 6 \times 3 \times 3$. Thereafter, CNS molecules were replaced randomly by DNS molecules, according to the given fraction X_{bulk}. In the case of S_{DNS}, a corresponding procedure was applied.

Calculation of the Mixing Energy (ΔE_{mix}). It is assumed that the lattice energy (E^{ideal}) of an *ideal* solid solution with molar fractions X_{bulk} and $(1 - X_{bulk})$ of DNS and CNS molecules, respectively, is given by a linear combination of the lattice energies of the pure crystal stuctures (E_{CNS} and E_{DNS}):

$$E^{ideal} = (1 - X_{bulk})E_{CNS} + X_{bulk}E_{DNS}$$

The excess of energy induced by the mixing of the two components CNS and DNS in the solid solutions (S^i), with $i =$ CNS or DNS, is thus

$$\Delta E^i_{mix} = E^{S_i} - E^{ideal}$$

where E^{S_i} denotes the lattice energies of the solid solution (S^i). ΔE^i_{mix} gives indications about the possibility of solid solution formation for the type of structure (S_i).

B. Generalized Markov Mean-Field Model. Growth along faces (*hkl*) is defined by a stacking of layers composed of buildings blocks, representing CNS molecules in state up, CNS molecules in state down, and nonpolar DNS molecules, respectively. In the case of the CNS/DNS system, two sites with different neighborhoods are present on the faces (*hkl*) considered. Therefore, separate molar fractions of CNS molecules in the up state (X^g_u), CNS molecules in the down state (X^g_d), and nonpolar DNS molecules (X^g_n) had to be taken into account for the two sites $g =$ I, II.

The layer-by-layer growth assumes the attachment and thermal relaxation with respect to the states up, down, and nonpolar of complete layers of molecules (adlayers), while formerly grown layers are kept frozen. Growth is taking place from the gas phase, providing a reservoir with constant molar fractions X_{gas} of DNS molecules and $(1 - X_{gas})$ of CNS molecules. Further on, it is assumed that crystal growth occurs near thermal equilibrium; that is, the time needed for the attachment of a new layer is much larger than the surface relaxation time.

The molar fractions X^g_u, X^g_d, and X^g_n (with $g =$ I, II) in the asymptotic state are obtained by the following equations of consistency

$$\begin{pmatrix} X^g_d \\ X^g_u \\ X^g_n \end{pmatrix} = \begin{pmatrix} P^g_d & P^g_d & P^g_d \\ P^g_u & P^g_u & P^g_u \\ P^g_n & P^g_n & P^g_n \end{pmatrix} \begin{pmatrix} X^g_d \\ X^g_u \\ X^g_n \end{pmatrix}$$

which have to be solved numerically; see ref 15. P^g_s is the attachment probability that a molecule in state $s = u$, d, or n (up, down, or nonpolar, respectively) will be attached to a surface site $g =$ I, II. On the basis of the assumption of thermal equilibrium formation of an adlayer, the probabilities P^g_s are given by normalized Boltzmann factors

$$P^g_s = \frac{1}{Z} x_s e^{-\beta f_s{}^g}$$

with

$$Z = \sum_s^{u,d,n} x_s e^{-\beta f_s{}^g}$$

and $x_s = 1 - X_{gas}$ if $s \in \{u, d\}$; otherwise, $x_s = X_{gas}$ if $s = n$. The term x_s originates from the chemical potentials of the two different components. Note that the chemical potentials in the gas and the solid are assumed to be the same; see ref 15.

f^g_s denotes the mean-field estimate of all the first nearest neighbor interactions involved between an attaching molecule in state s on surface site $g =$ I, II.

$$f^g_s = \sum_j^{u,d,n} X^g_j \sum_k E^k_{sj} + \sum_j^{u,d,n} X^{g'}_j \sum_l E^l_{sj}$$

with $s = u$, d, or n and $g =$ I, $g' =$ II and vice versa. The indices k and l refer to neighbors belonging to sites g and g', respectively.

References and Notes

(1) Polak, M.; Rubinovich, L. *Surf. Sci. Rep.* **2000**, *38*, 127−194.
(2) Drossel, B.; Kardar, M. *Phys. Rev. E* **1997**, *55*, 5026−5032.
(3) Dowden, P. A. *Surface Segregation Phenomena*; CRC Press: Boston, MA, 1990.
(4) Rodriguez, J. A. *Surf. Sci. Rep.* **1996**, *24*, 225−287.
(5) Vaida, M.; Shimon, J. W.; Weisinger-Lewin, Y.; Frolow, F.; Lahav, M.; Leizerowitz, L.; McMullan, R. *Science* **1988**, *241*, 1475.
(6) Weissbuch, I.; Addadi, L.; Lahav, M.; Leiserowitz, L. *Science* **1991**, *253*, 637−645.
(7) Weissbuch, I.; Popovitz-Biro, R.; Lahav, M.; Leiserowitz, L. *Acta Crystallogr., Sect. B* **1995**, *51*, 115−148.
(8) Weissbuch, I.; Lahav, M.; Leiserowitz, L. *Chem. Mater.* **1989**, *1*, 114−118.
(9) Hulliger, J. *Z. Kristallogr.* **1999**, *214*, 9−13.
(10) Hulliger, J. *Encyclopedia of Supramolecular Chemistry*; Atwood, J. L.; Steed, J. W., Eds.; Marcel Dekker: New York, 2004; pp 1120−1128.
(11) Hulliger, J.; Bebie, H.; Kluge, S.; Quintel, A. *Chem. Mater.* **2002**, *14*, 1523−1529.
(12) Bebie, H.; Hulliger, J.; Eugster, S.; Alaga-Bogdanovic, M. *Phys. Rev. E* **2002**, *66*, 021605.
(13) Gervais, C.; Wüst, T.; Behrnd, N.-R.; Wübbenhorst, M.; Hulliger, J. *Chem. Mater.* **2005**, *17*, 85−94.
(14) Kluge, S.; Dohnke, I.; Budde, F.; Hulliger, J. *CrystEngComm* **2003**, *5*, 67−69.
(15) Wüst, T.; Hulliger, J. *J. Chem. Phys.* **2005**, *122*, 084715.
(16) Gervais, C.; Grimbergen, R.; Markovits, I.; Ariaans, G.; Kaptein, B.; Bruggink, A.; Broxterman, Q. *J. Am. Chem. Soc.* **2004**, *126*, 655−662.

(17) Williams, E. J. *Proc. R. Soc. London, Ser. A* **1935**, *152*, 231−252.
(18) Gorsky, V. *Z. Phys.* **1928**, *50*, 64.
(19) Sun, H. *J. Phys. Chem. B* **1998**, *102*, 7338−7364.
(20) Kitaigorodsky, A. I. *Mixed Crystals*; Springer-Verlag: 1984; Chapter 4, pp 86−91.
(21) Wüst, T.; Gervais, C.; Hulliger, J. *Cryst. Growth Des.* **2005**, *5*, 93−97.
(22) Kitaigorodsky, A. I. *Mixed Crystals*; Springer-Verlag: 1984; Chapter 2, pp 17−48.